JAERI-M
5583

MHD STABILITY OF BELT-PINCH TYPE PLASMAS

February 1974

Masahiro WAKATANI

日本原子力研究所
Japan Atomic Energy Research Institute

この報告書は，日本原子力研究所が JAERI-M レポートとして，不定期に刊行している研究報告書です．入手，複製などのお問合わせは，日本原子力研究所技術情報部（茨城県那珂郡東海村）あて，お申しこしください．

JAERI-M reports, issued irregularly, describe the results of research works carried out in JAERI. Inquiries about the availability of reports and their reproduction should be addressed to Division of Technical Information, Japan Atomic Energy Research Institute, Tokai-mura, Naka-gun, Ibaraki-ken, Japan.

JAERI-M 5583

MHD Stability of Belt-Pinch Type Plasmas

Masahiro WAKATANI

Thermonuclear Fusion Laboratory, Tokai, JAERI

(Received February 1, 1974)

The stability of kink-like modes in the toroidal plasmas with hollow cylindrical geometry has been studied by means of their growth rate. The configurations simulate the tokamak with non-circular cross section elongated vertically or the " Belt-Pinch " type configuration. It is possible to increase the current in the toroidal plasmas of non-circular cross section with large axial length. The stability properties, however, are similar to those in the cylindrical plasma column.

JAERI—M 5583

ベルト型ピンチプラズマのＭＨＤ安定性

日本原子力研究所東海研究所核融合研究室

若谷誠宏

（１９７４年２月１日受理）

２つの同心円筒にかこまれているプラズマの平衡配位を求め，それがＭＨＤ的に安定かどうかを，ノーマルモードの成長率を計算することによって調べた。この平衡配位は，縦長の楕円断面をもったトカマクやベルト型ピンチの平衡配位を単純化したモデルになっている。このような非円形断面をもったトロイダルプラズマにおいて，軸方向の長さが大きいとき，電流を増加させることが可能である。しかしながら，安定性の性質は，円筒プラズマ柱の場合のものによく似ている。

目　次　な　し

§1. INTRODUCTION

The experiments of tokamaks with circular magnetic surface have been investigated and their macroscopic stability is consistent with MHD stability theory.[1)~3)] It shows that poloidal beta (β_p) must be lower than R/a to ensure equilibrium[4)] and safty factor (q) must be larger than 1,[5)] where R denotes major radius of a toroidal plasma and a denotes minor radius. These criterions limit beta ratio, $\beta = \beta_p (a/Rq)^2 < a/R$. In experiments stable discharges of tokamaks with $\beta_p \lesssim 1$ and $q \gtrsim 2$ have been obtained.

As a new possibility for increasing the current density and enhancing ohmic heating, discharges with non-circular plasma cross section have been under experimental[6)] and theoretical study.[7)] Toroidal plasma confinement, where the minor cross section of plasma is of a very elongated form in the direction of the main axis, encounters increasing attention, since experimental devices like the "Belt-Pinch"[8)] and the "Doublet"[9)] have given promising results.

A number of theoretical study on toroidal plasmas with non-circular cross sections have been reported. It has been shown that the stability against localized perturbations could be improved as well as the maximum equilibrium plasma pressure.[7)] Kink modes have received attention because they are commonly thought to be responsible for the impossibility to raise the current density.

In this paper, we study the stability of kink modes in the toroidal plasmas with the following model equilibria. The toroidal plasma with the elongated cross section is assumed to be a cylindrical plasma sheet of finite thickness within two annular conducting wall. The magnetic fields have axial and toroidal components, B_Z and B_θ respectively, where the cylindrical coordinate (R, θ, Z) has been used. The irreguralities given by the top and bottom ends of a finite structure may be neglected if the height of the conducting casing is large compared with the radial width of the casing.[10),11)] In this geometry the perturbations are fourier analyzed as $\exp(in\theta - ikZ)$.

where θ refers to the toroidal direction and Z to the poloidal direction.

The results obtained by this simplified model may explain the stability of kink modes in the "Belt-Pinch" type equilibrim. We compare our results with that obtained by Laval et al.[9] They dealt with more realistic, but also more complex axisymmetric models and considered geometrical variation in two dimensions.

In §2, the methods to obtain equilibria of hollow cylindrical plasmas are given and in §3 we briefly discuss the MHD stability using energy principle. In §4 the growth rates of kink modes are calculated as the eigen value problem of the linearized MhD equations. Finally the results obtained are discussed.

§2. COORDINATES AND EQUILIBRIUM

The equilibrium of sheet plasma with finite thickness which has two components of magnetic field, the longitudinal one created by external current, the axial one produced by an induced longitudinal current in the plasma, is considered in this section. It is bounded by metalic walls. The configuration is described by Fig. 1. The equilibrium equation in this coordinates is written as

$$\frac{\partial^2\psi}{\partial R^2} - \frac{1}{R}\frac{\partial\psi}{\partial R} + b_1(b_0 + b_2\psi) + aR^2 = 0 \ . \qquad (2.1)$$

Here we assumed $P = a(\psi - \psi_S)$ and $RB_\theta = b_0 + b_1\psi$, where ψ_S denotes ψ at the plasma surface and a, b_0 and b_1 are constants. The solution of eq. (2.1) is given by

$$\psi_P = -\frac{a}{b_1^2}R^2 - \frac{b_0}{b_1} + \{C_1J_1(b_1R) + C_2Y_1(b_1R)\}\ R \ , \qquad (2.2)$$

where J_1 and Y_1 are Bessel functions of first order and C_1, C_2 are constants. From this solution, we can find magnetic field,

$$RB_R = -\frac{\partial\psi}{\partial Z} = 0 \ , \qquad (2.3)$$

$$RB_Z = \frac{\partial\psi}{\partial R} = \frac{2a}{b_1^2}R + \{C_1J_1(b_1R) + C_2Y_1(b_1R)\} + \{C_1J_1'(b_1R) + C_2Y_1'(b_1R)\}\ b_1R \ , \qquad (2.4)$$

and current density,

$$J_\theta = \frac{2a}{b_1^2} + 2\{C_1J_1'(b_1R) + C_2Y_1'(b_1R)\}\ b_1 + \{C_1J_1''(b_1R) + C_2Y_1''(b_1R)\}\ b_1^2R \ , \qquad (2.5)$$

$$J_Z = -\frac{2a}{b_1} + \{C_1J_1'(b_1R) + C_2Y_1'(b_1R)\}\ b_1 + \{C_1J_1(b_1R) + C_2Y_1(b_1R)\}/R \ . \qquad (2.6)$$

When $a = 0$ and $b_1 = 0$ in eq. (2.1), the solution in the vacuum region is obtained in the form

$$\psi_V = D_1 + D_2 \frac{R^2}{2} , \tag{2.7}$$

where D_1 and D_2 are constants. The equilibrium considered here has two vacuum regions. The one exists between the inner conducting wall ($R = R_I$) and the plasma sheet and the other exists between the outer conducting wall ($R = R_0$) and the plasma sheet.

The constants C_1, C_2, D_1 and D_2 are determined by the boundary conditions. We denote the inner edge of the plasma sheet as $R = R_1$ and the outer edge as $R = R_2$ respectively. Then the boundary conditions are

$$\psi_V(R_0) = 0, \quad \psi_V(R_I) = 0 ;$$

$$\psi_V(R_1) = \psi_P(R_1), \quad \psi_V(R_2) = \psi_P(R_2);$$

$$\left.\frac{\partial \psi_V}{\partial R}\right|_{R=R_1} = \left.\frac{\partial \psi_P}{\partial R}\right|_{R=R_1}, \quad \left.\frac{\partial \psi_V}{R}\right|_{R=R_2} = \left.\frac{\partial \psi_P}{\partial R}\right|_{R=R_2}, \tag{2.8}$$

where the suffix V denotes the vacuum region and the suffix P denotes the plasma region.

Eqs. (2.2), (2.7) and the boundary conditions (2.8) determine equilibrium configurations of the cylindrical plasma sheet ($R_1 \leq R \leq R_2$) within the metalic casing ($R = R_I$ and $R = R_0$). Various equilibrium configurations are obtained by changing parameters a, b_0 and b_1. We devised the numerical procedure shown in Fig. 2 to calculate equilibrium configurations. The quantities characterizing equilibrium configurations are compression ratio $(R_0 - R_I)/(R_2 - R_1)$, beta ratio defined by

$$\beta = \frac{2\int_{R_1}^{R_2} PRdR}{\int_{R_1}^{R_2} (B_z^2 + B_\theta^2)RdR} \tag{2.9}$$

and the ratio of B_Z to B_θ at $R = R_2$.

Fig. 3 and Fig. 4 show examples of equilibria obtained by the above mentioned method. Fig. 3 shows the "Belt-Pinch" type configuration with high β and small compression ratio and Fig. 4 shows fairly low β equilibrium which may correspond to tokamak equilibrium with elongated plasma cross section.

In §4, we will use these equilibrium configurations to calculate the growth rates of MHD kink modes.

§3. MHD STABILITY CONSIDERATION

The stability of the model equilibrium shown in §2 is determined by the stability analyses similar to that of cylindrical plasmas. In stability theory the position of the singular point, $R = R_S$, which satisfy the relation

$$kR_S B_Z(R_S) = nB_\theta(R_S) \tag{3.1}$$

makes an essential role. Therefore we firstly see pitch profile of the typical equilibrium in Fig. 5. Here the pitch is defined by RB_Z/B_θ. It is noted that the pitch profile has maximum at the inner edge of the plasma column. By choosing the set (n, k), it will be possible to have two singular points. We will devide the equilibrium configuration into three regions and discuss the MHD stability qualitatively.

The well known energy principle[12] can be written in the form,

$$W = \frac{\pi}{2}\int_{R_I}^{R_O} \{ \frac{1}{n^2+k^2k^2} [(kRB_Z-nB_\theta)\frac{d\xi}{dR} + (kRB_Z+nB_\theta)\frac{\xi}{R}]^2$$

$$+ [(kRB_Z-nB_\theta)^2 - 2B_\theta \frac{d}{dR}(RB_\theta)]\frac{\xi^2}{R^2}\} RdR , \tag{3.2}$$

when minimization about ξ_θ and ξ_Z have been carried out. Here the displacement $\vec{\xi}$ is given by

$$\vec{\xi} = \Sigma\, \vec{\xi}(R)\exp(in\theta - ikZ) \tag{3.3}$$

and ξ denotes ξ_R. Integrating the term $\xi\, \xi\, d/dR$ in eq. (3.2) by the partial integration, we obtain

$$W = W_f + W_a + W_e, \tag{3.4}$$

where

$$W = \frac{\pi}{2}\int_{R_1}^{R_2} [\, f(\frac{d\xi}{dR})^2 + g\xi^2\,]\, dR, \tag{3.5}$$

$$W_a = \frac{\pi}{2}\left(\frac{k^2R_2^2B_Z^2(R_2) - n^2B_\theta^2(R_2)}{n^2 + k^2R_2^2}\xi(R_2)^2 - \frac{k^2R_1^2B_Z^2 - n^2B_\theta^2(R_1)}{n^2 + k^2R_1^2}\xi(R_1)^2\right) \tag{3.6}$$

$$W_e = \frac{\pi}{2}\left(\int_{R_1}^{R_1} + \int_{R_2}^{R_0}\right)\left[\frac{R}{4\pi}\frac{(nB_\theta - kRB_Z)^2}{n^2+k^2R^2}\left(\frac{d\xi}{dR}\right)^2\right.$$

$$\left. + \left\{\frac{1}{4\pi R}(nB_\theta - kRB)^2\frac{k^2R^2+n^2-1}{n^2+k^2R^2} + \frac{2k^2R}{4\pi(n^2+k^2R^2)}(k^2R^2B_Z^2 - n^2B_\theta^2)\right\}\theta^2\right]dR, \tag{3.7}$$

$$f = \frac{R}{4\pi}\frac{(nB_\theta - kRB_Z)^2}{n^2+k^2R^2} \tag{3.8}$$

and

$$g = \frac{2k^2R^2}{n^2+k^2R^2}\frac{dP}{dR} + \frac{1}{4\pi R}(nB_\theta - kRB_Z)^2\frac{k^2R^2+n^2-1}{n^2+k^2R^2}$$

$$+ \frac{2k^2R^2}{4\pi(n^2+k^2R^2)^2}(k^2R^2B_Z^2 - n^2B_\theta^2) \quad . \tag{3.9}$$

When the singular point exists in $R_m < R < R_2$ (R_m means the magnetic axis), energy integral in the vacuum region, W_e, is non-negative. As $g(R_S) < 0$, it is possible that an unstable mode localized arround $R = R_S$ appears. Therefore we study only the energy integral, W_f, to know the stability of this mode. We expand f around $R = R_S$,

$$f = f_1(R_S)(R - R_S)^2 \quad . \tag{3.10}$$

When the well-known inequality, $\int x^2(d\xi/dx)^2dx \geq 1/4\int \xi^2dx$, is applied

$$W_f \geq \frac{\pi}{2}\int \tilde{g}(R)\,\xi^2dR \tag{3.11}$$

is obtained, where $\tilde{g}(R) \equiv g(R) + 1/4\ f_1(R_S)$. The stability condition reduces to $\tilde{g}(R) > 0$ around $R = R_S$. The sufficient

stability condition is obtained

$$\frac{q'^2}{4q^2}R^2\left(1-\frac{4n^2B_\theta^2}{DB_2^2}\right)+\frac{8\pi RP'}{B_Z^2}\left(1+\frac{q'^2R^2}{4q^2}\frac{n^2B^2}{DB_Z^2}\right)-\frac{4n^2B_\theta^4}{DB^4}>0, \tag{3.12}$$

$$D=n^2(n^2-1)+(2n^2+1)n^2\frac{B_\theta^2}{B_Z^2}+n^4\frac{B_\theta^4}{B_Z^4},$$

from the minimum value of $\tilde{g}(R)$. If $B_\theta \gg B_Z$ is used,

$$\frac{q'^2}{4q^2}+\frac{8\pi P'}{B_Z^2R}>0 \tag{3.13}$$

is obtained. This condition is the well-known Suydam condition. From Fig. 5, we know the shear term (the first term of (3.13)) is large in $R_m<R<R_2$ and the condition (3.13) may be satisfied. Even if this unstable mode is excited in the plasma column, the growth rate may be smaller than the mode having the singular point in the vacuum region, $R_2\leq R\leq R_0$, as discussed later.

Next we consider the case $R_1\leq R_S\leq R_m$. In the vacuum retion $J_Z=0$ and in $R_1<R<R_m$, J_Z is negative as is shown in Fig. 3 or Fig. 4. From eq. (3.2), the region where $J_ZB_\theta<0$ gives positive contribution to the energy integral. Due to impossibility of localization, an unstable mode may not appear.

Lastly we consider the case $R_2\leq R_S\leq R_0$. As the singular point exists in the vacuum region, a kink-like mode which disturb the whole plasma column may be excited. The Euler equation.

$$\frac{d}{dR}f\frac{d\xi}{dR}-g\xi=0 \tag{3.14}$$

is obtained from the energy integral in the plasma region. From this equation,

$$\frac{d\xi}{dR}=\frac{1}{f}\int_{R_1}^{R}gdR+\left.\frac{d\xi}{dR}\right|_{R=R_1} \tag{3.15}$$

is derived. Because of the condition $R_2 \leq R_S \leq R_0$, $f \neq 0$ and $\int_{R_1}^{R} g dR > 0$ is valid. Also $d\xi/dR|_{R=R_1}$ is usually positive. Thus $\xi(R_1)$ is smaller than $\xi(R_2)$. From this relation and $n^2 B_\theta^2(R_2) > k^2 R_2^2 B_Z^2(R_2)$ (which ensures $R_2 \leq R_S \leq R_0$), $W_a < 0$ is obtained. This means that an unstable mode distorting the edge of the plasma column can appear. We consider that this mode is most dangerous to the equilibrium configuration shown in §2, and we will carry out the stability analysis intensively in §4.

We will note the stability of n = 0 mode. The potential energy for n = 0 is written in the form

$$W = \frac{\pi}{2} \int_{R_I}^{R_0} \{ B_Z^2 \left(\frac{d\xi}{dR} + \frac{\xi}{R} \right)^2 - 2B_\theta \frac{d}{dR}(RB_\theta) \frac{\xi^2}{R^2} \} RdR$$

$$+ k^2 \frac{\pi}{2} \int_{R_I}^{R_0} RB^2 \xi^2 dR \quad . \tag{3.16}$$

As the second term is positive definite, the equilibrium is stable if $W > 0$ for $k \to k_{min.}$. In §4, we will calculate the growth rate of n = 0 mode for $k = k_{min.}$

§4. GROWTH RATE OF MHD KINK MODES

In this section, we calculate the growth rate of MHD kink modes, which have a singular point in the external vacuum region as discussed in §3. We have used the linearized MHD equations in the cylindrical geometry derived by Hain and Lüst,

$$\left[\frac{(\omega^2\rho + F^2)\{\omega^2\rho(\gamma P + B^2) + \gamma PF^2\}}{N}\frac{1}{R}(R\xi)'\right]'$$

$$+\left[-\omega^2\rho - F^2 - 2B_\theta\left(\frac{B_\theta}{R}\right)' + \frac{4k^2B_\theta^2}{R}\cdot\frac{(\rho\omega^2B^2 + \gamma F^2)}{N}\right.$$

$$\left.+ R\left\{\frac{2kB_\theta(mB_Z/R + kB_\theta)}{R^2}\cdot\frac{(\omega^2\rho(\gamma P + B^2) + \gamma PF^2)}{N}\right\}'\right]\xi = 0, \tag{4.1}$$

where

$$N = \omega^4\rho^2 + \omega^2\rho G(\gamma P + B^2) + G\gamma PF^2$$

$$F = nB_\theta/R - kB_Z$$

and $$G = k^2 + n^2/R^2 \quad .$$

Here the prime denotes the derivative with respect R.
We obtain the growth rate ω as the eigenvalue problem, using the boundary conditions

$$\left.\begin{aligned} &b_R(R_I) = 0, \quad b_R(R_0) = 0 \ , \\ &b_R(R_1) = i\left(\frac{m}{R}B_\theta - kB_Z\right)\xi\Big|_{R=R_1}, \\ &b_R(R_2) = i\left(\frac{m}{R}B_\theta - kB_Z\right)\xi\Big|_{R=R_2} \ , \end{aligned}\right\} \tag{4.2}$$

and the equality of the pressures at R_1 and R_2.[14]
Here b_R denotes the perturbed magnetic field given by

$$ib_R = C_1 I_m'(kr) + C_2 K_m'(kr) \quad , \tag{4.3}$$

where I_m and K_m denote modified Bessel functions. Fig. 6 shows growth rate of kink-like mode in the equilibrium configurations in Fig. 3 which has a fairly large β, $\beta \simeq 77\%$, and in Fig. 4 which has $\beta \simeq 11\%$. The growth rates have been calculated by varing k, which means that the mode with an arbitrary value can appear. The unstable values of k show the discrete bands according to the mode number n = 1, 2, 3. This results may be expanined by the fact that an unstable kink-like mode appears for $R_2 < R_S \leq R_0$. This figures also shows that the growth rate is greater for large n. The growth rate normalized by

$$\omega_0 = B_Z(R_2)/\sqrt{\rho(R_m)}\ (R_2-R_1) \tag{4.4}$$

seems to be large for the low β equlibrium, but the growth rate ω is small due to large Alfvén velocity. Fig. 7 shows the growth rates for the case with the large compression ratio. The region of unstable k value becomes wider. The extension of the vacuum region may explain this result. Considering that ω_0 is proportion to $(R_2-R_1)^{-1}$, we know that the growth rate dose not change drastically by the compression ratio.

Hereafter we consider the cylindrical plasma sheet has a finite length, L, along the Z axis. This restricts the wave number and the modes having discrete wave numbers, $k = mk_{min.}$, may be excited in the plasma sheet, where $k_{min.} = 1/L$. We will define the safty factor, q(R), as

$$q(R) = \frac{1}{kR}\frac{B_\theta(R)}{B_Z(R)} \quad , \tag{4.5}$$

and q_a as

$$q_a = \frac{L}{mR_2}\frac{B_\theta(R_2)}{B_Z(R_2)} \quad . \tag{4.6}$$

From (3.1) and (4.5), the singular point satisfies

$$q(R_S) = \frac{m}{n} \quad . \tag{4.7}$$

When the ratio, $B_\theta(R_2)/B_Z(R_2)$, is varied, the position of the singular point is changed according to (4.7). From the above discussions, we have known that a kink-like mode may be excited if $R_2 < R_S \leq R_0$. When we calculate the growth rate of MHD kink mode for various values of $B_Z(R_2)/B_\theta(R_2)$, we obtain the stability diagram shown in Fig. 8, where the ordinate shows the normalized growth rate for n = 1 mode and the abscissa shows q_a. Here we note there is some ambiguity in this diagram, because it is difficult to separate out the parameter, $B_Z(R_2)/B_\theta(R_2)$, due to the coupling of the toroidicity with the conducting walls. Fig. 8 shows that the ranges of unstable q_a appear discretely when the toroidal current varies. It is noted that the stable region for m = 1 mode appears since we consider only n = 1 mode. This stability property is very similar to that of the usual cylindrical plasma column.[5),14)]

We discuss the effect of non-circular cross section on the stability. Here we consider the case that the cross section is deformed to the ellipse elongated along the Z axis. When we make L large, the value of $B_Z(R_2)$ becomes smaller for constant toroidal current. From (3.1), we find

$$R^2/L^2 \simeq B_\theta^0/mI \quad , \tag{4.8}$$

where we have used $B_\theta(R) = B_\theta^0/R$ and $B_Z(R) \simeq I/2L$.

As the right hand side in eq. (4.8) is constant, R satisfying (4.8) varies according to the length along the Z axis, L. This fact means that the singular point moves to large R when the elongation of ellipse become large. Fig. 9 shows the stability diagram where hatched regions are unstable. The ordinate denotes the toroidal current and the abscissa denotes the elongation of the ellipse. In (4.8) R is considered

R_2, and the following relation is obtained,

$$J \simeq \frac{I}{L^2} \simeq \frac{B_\theta^0}{m(R + \frac{S}{L})^2} \quad , \tag{4.9}$$

where $(R_1 - R_2)\, L = S = \text{const.}$ is assumed. From this relation the current density J is increased when L becomes large. This stability property is similar to that obtained by Laval et al.[9] For fixed $L/(R_2 - R_1)$, we again find the result shown in Fig. 8 that the range of unstable I appears discretely.

Lastly we add that the equilibrium configuration with which we calculate the growth rates, is stable to n = 0 mode for $k_{min.} = 0.003$. This axisymmetric mode, however, does not correspond to the positional instability. The lack of positional instability in our study comes from the infinite length along the Z axis.

Acknowledgement

The auther would like to thank to Dr. M. Tanaka for stimulating discussions and helpful advices.

References

1) L.A. Artsimovich et al.: Nucl. Fusion Special Suppl. (1969) 17.
2) D. Dimock et al.: in Fourth Conference on Plasma Physics and Controlled Nuclear Fusion Research (Madison), 1971, CN-28/C-9.
3) S. Itoh et al.: in Third International Symposium on Toroidal Plasma Confinement (Garching), 1973, B-4.
4) C. Mercier: Nucl. Fusion 3 (1963) 89.
5) V.D. Shafranov: Soviet- Physics Technical Phisics 15 (1970) 175.
6) T. Ohkawa et al.: in Sixth European Conference on Controlled Fusion and Plasma Physics (Moscow), 1972, P161.
7) M. Tanaka and T. Tuda: JAERI-M 4532 (1971).
8) W. Zwicker et al.: in Fourth Conference on Plasma Physics and Controlled Nuclear Fusion Research (Madison), 1971, CN-28/B-6.
9) G. Laval, R. Pellat and J.L. Soule: in Third International Symposium on Toroidal Plasma Confinement (Garching), 1973, F2-I.
10) W. Grossmann: in Second Topical Conference on Pulsed High Beta Plasmas (Munchen), 1972, F-9.
11) F. Hoffmann: Nucl. Fusion 13 (1973) 297.
12) W.A. Newcomb: Ann. Phys. 10 (1960) 232.
13) K. Hain and R. Lüst: Z. Naturforsh. 13a (1958) 936.
14) T. Amano, M. Wakatani and M. Watanabe: J. Phys. Soc. Japan 33 (1972) 782.

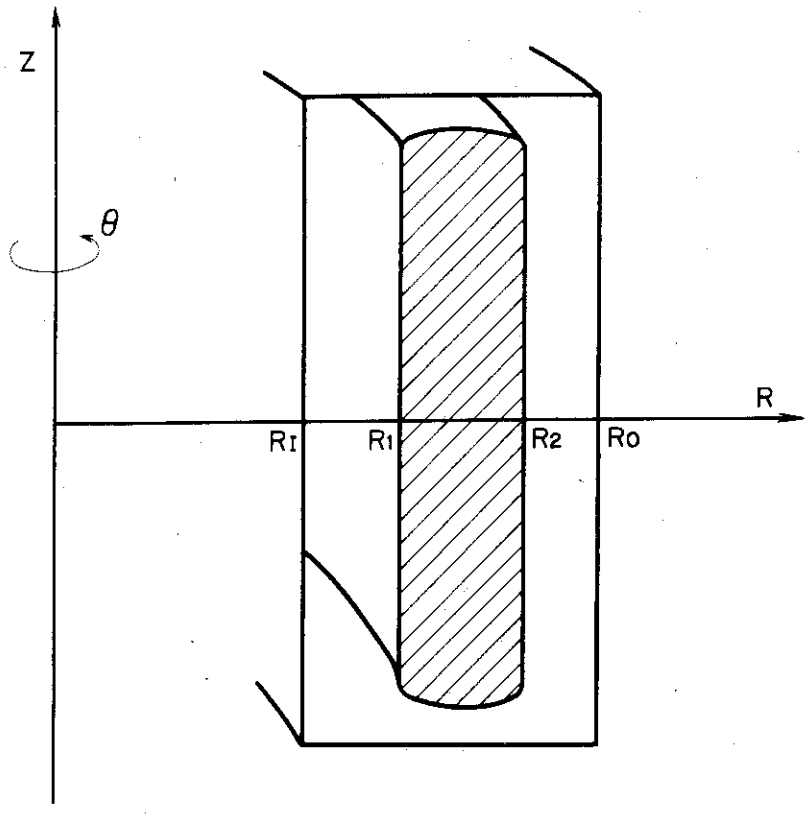

Fig. 1 The congiguration and the coordinates.

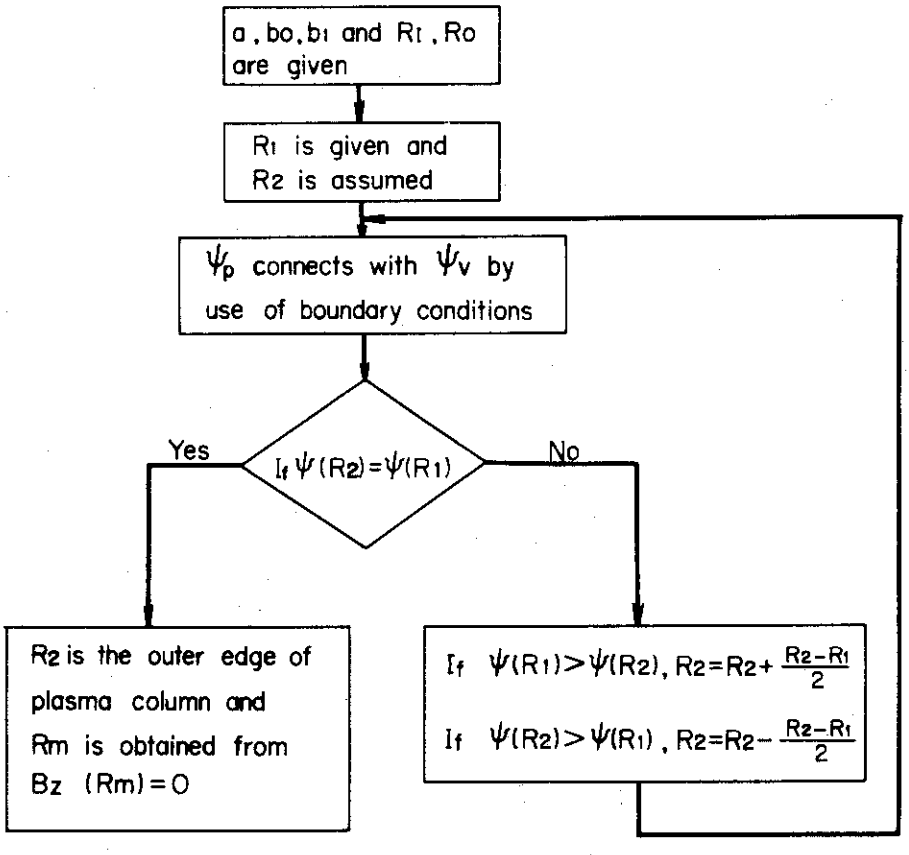

Fig. 2 The procedure of numerical calculations to obtain the equilibrium configuration.

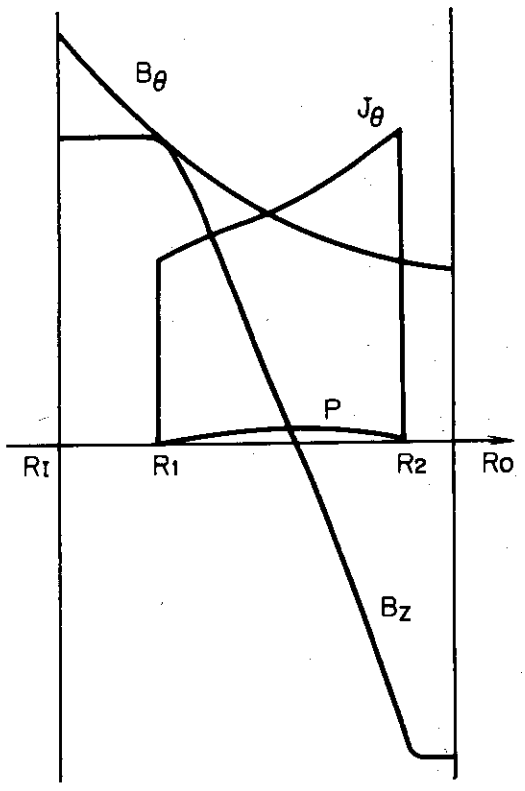

Fig. 3 Equilibrium configuration with $R_I = 3.0$, $R_1 = 4.0$, $R_2 = 6.48$, $R_0 = 7.0$ and $\beta = 77.5\%$ ($a = 0.01$, $b_0 = 0.25$ and $b_1 = 0.05$).

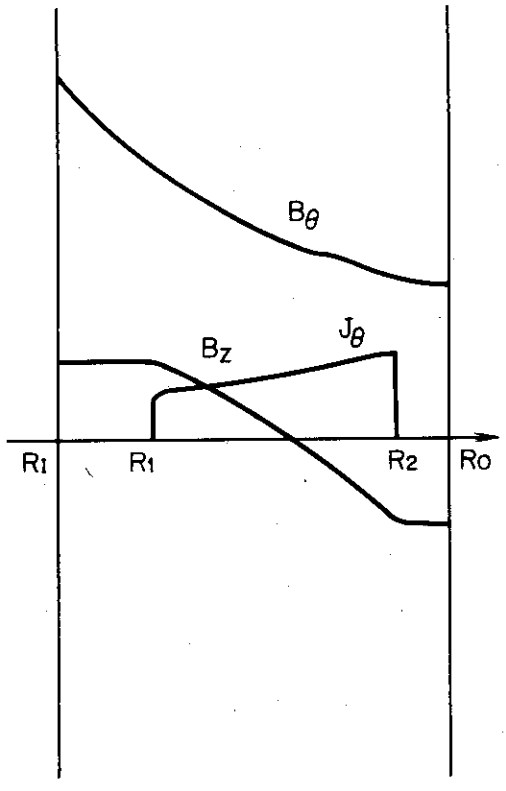

Fig. 4 Equilibrium configuration with $R_I = 3.0$, $R_1 = 4.0$, $R_2 = 6.51$, $R_0 = 7.0$ and $\beta = 11.7\%$ ($a = 0.01$, $b_0 = 0.75$ and $b_1 = 0.05$).

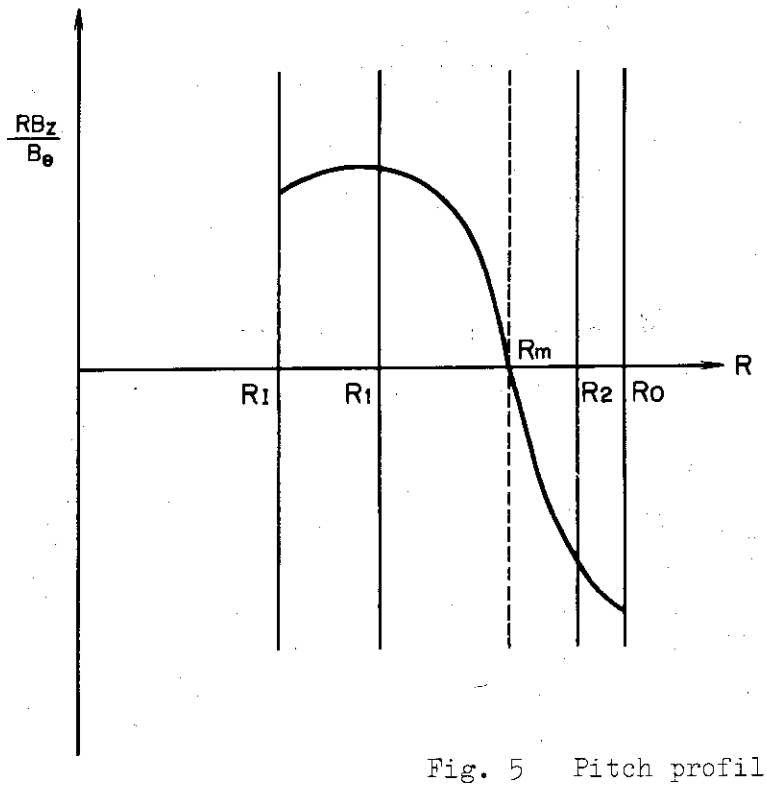

Fig. 5 Pitch profile.

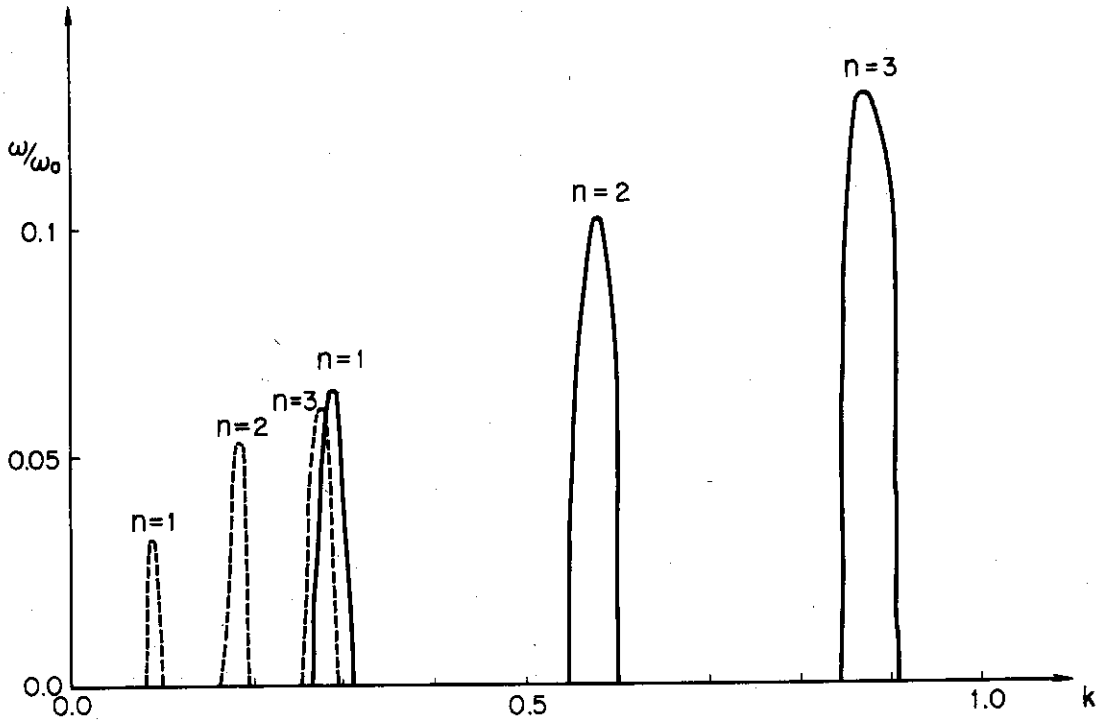

Fig. 6 Growth rates of kink-like modes with n = 1, 2, 3 in the equilibrium configuration shown in Fig. 3 and Fig. 4. The solid lines show those corresponding to Fig. 3 and the dashed lines show those coresponding to Fig. 4.

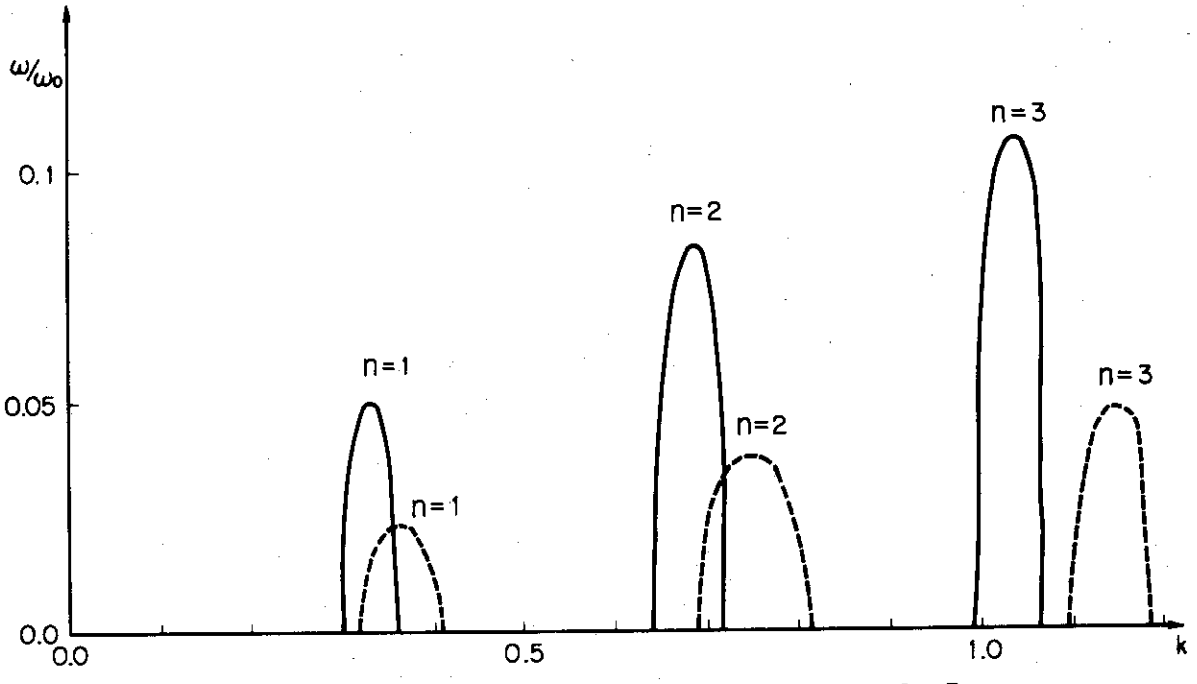

Fig. 7 Growth rates of kink-like modes with n = 1, 2, 3. The solid lines show those in the equilibrium configuration with R_I = 3.0, R_1 = 4.50, R_2 = 6.16, R_0 = 7.0 and β = 10.4% (a = 0.5, b_0 = 28.0 and b_1 = 0.05). The solied lines show those in the equilibrium configuration with R_I = 3.0, R_1 = 5.0, R_2 = 5.75, R_0 = 7.0 and β = 10.7% (a = 0.5, b_0 = 13.0 and b_1 = 0.05).

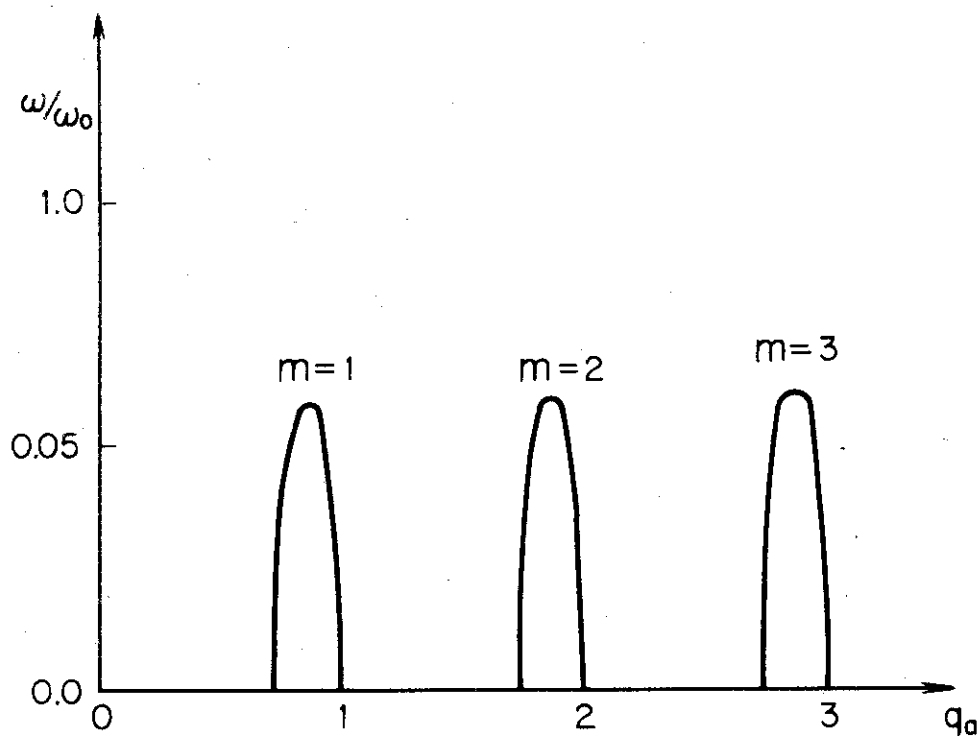

Fig. 8 Growth rates of kink-like modes with m = 1, 2, 3 and n = 1 versus q_a.

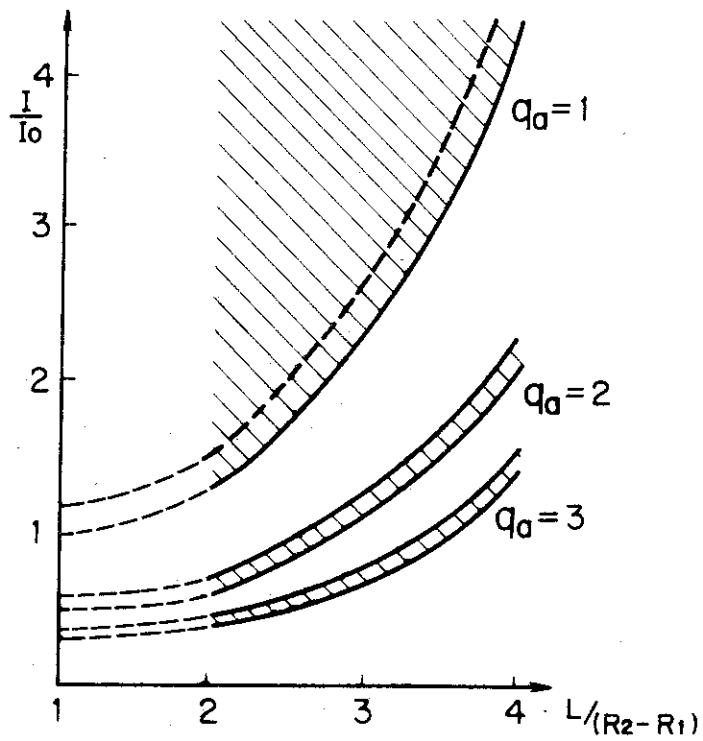

Fig. 9 Stability diagram in changing the height of conducting casing L. T
The dashed lines between 1 and 2 of the abscissa are not determined in this analysis and values at $L/(R_2-R_1) = 2$ are assumed to be known.